

Dark matter annihilation and non-thermal Sunyaev-Zel'dovich effect: I. galaxy cluster

Qiang Yuan, Xiaojun Bi

Key Laboratory of Particle Astrophysics, Institute of High Energy Physics, Chinese Academy of Sciences, Beijing 100049, China

Feng Huang, Xuelei Chen

National Astronomical Observatories, Chinese Academy of Sciences, 20A Datun Road, Beijing 100012, China

ABSTRACT: In this work we calculate the Sunyaev-Zel'dovich (SZ) effect due to the e^+e^- from dark matter (DM) annihilation in galaxy clusters. Two candidates of DM particle, (1) the weakly-interacting massive particle (WIMP) and (2) the light dark matter (LDM) are investigated. For each case, we also consider several DM profiles with and without central cusp. We generally find smaller signals than previously reported. Moreover, the diffusion of electrons and positrons in the galaxy clusters, which was generally thought to be negligible, is considered and found to have significant effect on the central electron/positron distribution for DM profile with large spatial gradient. We find that the SZ effect from WIMP is almost always non-observable, even for the highly cuspy DM profile, and using the next generation SZ interferometer such as ALMA. Although the signal of the LDM is much larger than that of the WIMP, the final SZ effect is still very small due to the smoothing effect of diffusion. Only for the configuration with large central cusp and extremely small diffusion effect, the LDM induced SZ effect might have a bit chance of being detected.

KEYWORDS: galaxies: clusters — cosmic microwave background — dark matter — Sunyaev-Zel'dovich effect.

Contents

1. Introduction	1
2. Gas and DM distributions in cluster	2
3. Electron/positron production from DM annihilation	4
3.1 WIMP	5
3.2 LDM	6
4. Propagation of electrons in cluster	6
4.1 The diffusionless approximation	7
4.2 The effect of diffusion	8
5. SZ effect	9
6. Discussion	12

1. Introduction

The Dark matter (DM) problem is one of the most important issues in modern physics and cosmology. After about eighty years since the first discovery of DM in the Coma cluster by Zwicky [1], the evidences of DM are overwhelming nowadays. However, most of the evidences come from the gravitational effects by astronomical observations, such as the rotation curve of spiral galaxies [2], dynamics of galaxy clusters [3], gravitational lensing effect [4], large scale structure of the universe [5] and the anisotropy of cosmic microwave background [6, 7, 8]. The studies on primordial nucleosynthesis [9, 10] and structure formation [11] show that most of the DM is *non-baryonic* and *cold*. The nature of DM particle is still unknown and remains as one of the biggest puzzles in physics and astronomy today.

Many candidates of DM have been proposed in literature (for reviews, see e.g. [12, 13]). Among the “zoo” of the DM candidates, the weakly-interacting massive particles (WIMP) are most favored since they appear naturally in many of the new physics models at the electroweak scale and can give the correct relic density of DM. The masses of WIMP are typically in the range of a few GeV to several TeV, and for weak scale interaction its relic density agrees roughly with observation [12]. The most popular example is neutralino, which is the lightest supersymmetric particle in the minimal supersymmetric extension of the standard model (MSSM). Typical mass of the neutralino can not be significantly lighter than a few GeV [14]. However, scenarios with light particles with mass from MeV

to GeV are also able to satisfy the constraints from relic density and other astrophysical observations [15, 16]. Furthermore, the light DM (LDM¹) annihilation was proposed to explain the 511 keV line emission from the bulge around the Galactic center [17]. Further studies from astrophysical constraints limited the parameter space of LDM in a narrow range [18, 19, 20, 21, 22, 23].

To identify the nature of DM particles, it is necessary to “see” them in particle physics experiments beyond the gravitational measurement. There are usually three types of experiments suggested to capture the DM particles: the *collider-based searches* to observe the missing energy in particle collisions, the *direct searches* to capture the scattering signals between DM particle and detector nucleus, and the *indirect searches* to measure the annihilation products in cosmic rays like γ -rays, anti-particles and neutrinos etc. (for a review see Ref. [12]).

It has been suggested that the inverse Compton (IC) scattering between electrons/positrons induced by DM annihilation and the CMB photon, which causes a non-thermal Sunyaev-Zel’dovich (SZ) effect on CMB, could be an alternative way for DM *indirect searches* [24, 25, 26, 27, 28]. The DM induced SZ effect shows a specific spectrum which differs from the usual thermal SZ effect, and can be isolated from other SZ effects with observations of arcmin angular resolution and μK sensitivity [28]. In this and a companion paper (paper II) we revisit the detectability of the DM induced SZ effect in two typical kinds of objects: the galaxy clusters (this paper) and dwarf galaxies (paper II). Both the WIMP and light candidate of DM particles are considered.

The outline of this paper is as follows. In Sec.2 we introduce the thermal gas distribution and DM configuration we adopted, and give the cluster sample we used in this work. The production of electrons/positrons from DM annihilation is presented in Sec.3, and the propagation of electrons/positrons in cluster is described in Sec.4. Sec.5 gives the results of the SZ effect calculations. Finally we draw the conclusions and some discussions in Sec.6. Throughout the paper, we assume a flat ΛCDM model, with the cosmological parameters of the Wilkinson Microwave Anisotropy Probe (WMAP) five year best fitted values, i.e. $\Omega_M = 0.28$, $\Omega_\Lambda = 0.72$ and Hubble constant $h = 0.7$ [8].

2. Gas and DM distributions in cluster

The galaxy cluster consists of fully ionized gas with temperature $1 \sim 10$ keV. The thermal electron distribution can be described using an isothermal β -model [29]

$$n_e(r) = n_{e0} \left(1 + \frac{r^2}{r_c^2} \right)^{-\frac{3\beta}{2}}, \quad (2.1)$$

where n_{e0} is the central number density of electrons, r_c is the core radius and β represents the square of ratio of the galaxy-to-gas velocity dispersions in the cluster [29, 30]. The

¹Here we give separate discussions about LDM and WIMP according to the usual conventions in the literature. However, it should be noted that the light DM might be a sub-class of WIMP DM with the only difference coming from that it does not suffer from the Lee-Weinberg limit, as emphasized in Refs. [15, 16].

isothermal β -model is well consistent with the X-ray observations and the parameters can be precisely determined from the X-ray surface brightness image of the cluster.

For the DM distribution in the cluster, however, the most precise knowledge comes from numerical simulations. N-body simulations show that there may be a nearly universal central cusp of DM density profile, though the exact slope near the center is still being debated [31, 32, 33, 34]. However, the observations of the rotation curves of galaxies favored cored DM distribution [35, 36, 37]. For a review of the DM halo properties please refer to Ref. [38]. In this work we will adopt the following three types of DM density profiles for discussion:

$$\rho(r) = \frac{\rho_s}{(1 + r/r_s)[1 + (r/r_s)^2]} \quad (\text{hereafter B95, Ref. [36]}), \quad (2.2)$$

$$\rho(r) = \frac{\rho_s}{(r/r_s)(1 + r/r_s)^2} \quad (\text{hereafter NFW, Ref. [31]}), \quad (2.3)$$

$$\rho(r) = \frac{\rho_s}{(r/r_s)^{1.5}[1 + (r/r_s)^{1.5}]} \quad (\text{hereafter M99, Ref. [39]}). \quad (2.4)$$

There are some other profiles with different inner slopes also proposed in literatures [32, 33, 34]. Most of these results show similar behaviors ($\sim r^{-3}$) at large radius, but show discrepancies in the inner region of the halo. Here we employ B95, NFW and M99 profiles as prototypes of non-cuspy, mediately cuspy and strongly cuspy profiles of DM halos respectively.

Physically, however, the density of DM halo should not diverge, so we introduce a cutoff radius within which the density is kept at constant ρ_{\max} , probably due to balance between the annihilating rate and the in-falling rate of DM [40]. Typically we have $\rho_{\max} = 10^{18} \sim 10^{19} \text{ M}_\odot \text{ kpc}^{-3}$ [41], and we fix $\rho_{\max} = 10^{18} \text{ M}_\odot \text{ kpc}^{-3}$ in this work.

The profile parameters ρ_s and r_s are determined using the virial mass M_{vir} and concentration parameter c_{vir} of the DM halo [42]. The virial radius of a DM halo is defined as

$$r_{\text{vir}} = \left(\frac{M_{\text{vir}}}{(4\pi/3)\Delta\rho_c(z)} \right)^{1/3}, \quad (2.5)$$

where Δ is the overdensity, and $\rho_c(z)$ is the critical density of the universe at the redshift of the cluster. For Λ CDM universe, $\Delta \approx 18\pi^2 + 82x - 39x^2$ with $x = \Omega_M(z) - 1 = -\frac{\Omega_\Lambda}{\Omega_M(1+z)^3 + \Omega_\Lambda}$ is found to be a good approximation [43]. The concentration parameter c_{vir} is defined as

$$c_{\text{vir}} = \frac{r_{\text{vir}}}{r_{-2}}, \quad (2.6)$$

where r_{-2} refers to the radius at which $\frac{d(r^2\rho)}{dr}|_{r=r_{-2}} = 0$. The concentration parameter c_{vir} relates r_{vir} and the density profile parameter as [42]

$$r_s^{\text{B95}} = \frac{r_{\text{vir}}}{1.52c_{\text{vir}}}, \quad r_s^{\text{NFW}} = \frac{r_{\text{vir}}}{c_{\text{vir}}}, \quad r_s^{\text{M99}} = \frac{r_{\text{vir}}}{0.63c_{\text{vir}}}. \quad (2.7)$$

Therefore if the $c_{\text{vir}} - M_{\text{vir}}$ relation is specified, r_s is determined using Eq.(2.7), and then ρ_s can be derived by mass condition $\int \rho(r)dV = M_{\text{vir}}$. Generally the $c_{\text{vir}} - M_{\text{vir}}$ relation

Table 1: The β -model parameters of thermal electron distribution and total virial mass of the cluster sample.

Name	z	$n_{e0}(\text{cm}^{-3})$	$\theta_c(\text{arcsec})^1$	β	$kT(\text{keV})$	$M_{\text{vir}}(10^{14}M_{\odot})$	Ref. ²
Abell 1060	0.011	3.19×10^{-3}	441	0.70	3.28	4.40	[46] [47]
Abell 262	0.016	7.25×10^{-3}	87	0.39	1.45	2.70	[46] [47]
Coma	0.023	3.42×10^{-3}	624	0.75	7.80	12.9	[48] [49]
Abell 2199	0.030	9.90×10^{-3}	132	0.61	3.13	7.00	[46] [47]
Abell 496	0.033	5.04×10^{-3}	194.4	0.64	6.34	5.20	[46] [47]
Abell 2717	0.049	9.60×10^{-3}	35.5	0.48	1.64	1.92	[50] [51]
Abell 1795	0.063	2.45×10^{-2}	45	0.57	6.74	9.07	[46] [52]
Abell 478	0.088	2.36×10^{-2}	50.4	0.62	8.32	16.0	[46] [52]
PKS0745-191	0.103	5.50×10^{-2}	24.6	0.57	7.70	11.9	[53] [51]

¹ θ_c connects with the core radius r_c by the angular radius d_A as $\theta_c \approx r_c/d_A$.

²The former reference is for the gas distribution and temperature, while the latter one is for the mass. The mass is actually adopted from the compilation of Ref. [45], where the correction of different cosmological models are made. The one listed is the original reference.

should be inferred from the numerical simulations[42, 44]. In this work we adopt the fitting observational $c_{\text{vir}} - M_{\text{vir}}$ relation [45]

$$c_{\text{vir}} = \frac{14.5}{1+z} \left(\frac{M}{M_{\star}} \right)^{-0.15}, \quad (2.8)$$

where the reference mass $M_{\star} = 1.3 \times 10^{13} h^{-1} M_{\odot}$.

We compiled a sample of 9 nearby clusters with redshift $z \lesssim 0.1$ to discuss the non-thermal SZ effect from DM annihilation in this work. The β -model parameters and virial mass are given in Table 1. Since the basic properties of the SZ effects are similar for different clusters, we will use the Coma cluster as the prime example to introduce the calculation process. The results from all of the clusters are presented last.

3. Electron/positron production from DM annihilation

The production, propagation and scattering with photons are the same for the electrons and the positrons in the current work, so for simplicity we will only discuss electrons in the following. The final resulting SZ effect are multiplied by a factor 2 to account for the contributions from positrons. The electron source function from DM annihilation can be written as

$$Q_e(E, \mathbf{r}) = \frac{\langle \sigma v \rangle}{2m_{\chi}^2} \frac{dN}{dE} \rho^2(\mathbf{r}), \quad (3.1)$$

where $\langle \sigma v \rangle$ is the velocity-weighted annihilation cross section, m_{χ} is the mass of DM particle, dN/dE is the electron yield spectrum per annihilation, and $\rho(\mathbf{r})$ is the density of DM. In this work we consider two types of DM particles: WIMP and LDM.

3.1 WIMP

Neutralino is taken as an example of WIMP DM. The direct channel to e^+e^- is suppressed for neutralino, so electrons are in most cases produced in the cascades of the annihilation final-state particles such as heavy leptons, quarks and gauge bosons [13]. The spectra of electrons can be different from each other for different annihilation modes. We use the package DarkSUSY [54] to calculate the cross section and final-state spectra of electrons. In Figure 1 we plot the electron yield spectra for three typical modes of neutralino annihilation: W^+W^- , $b\bar{b}$ and $\tau^+\tau^-$.

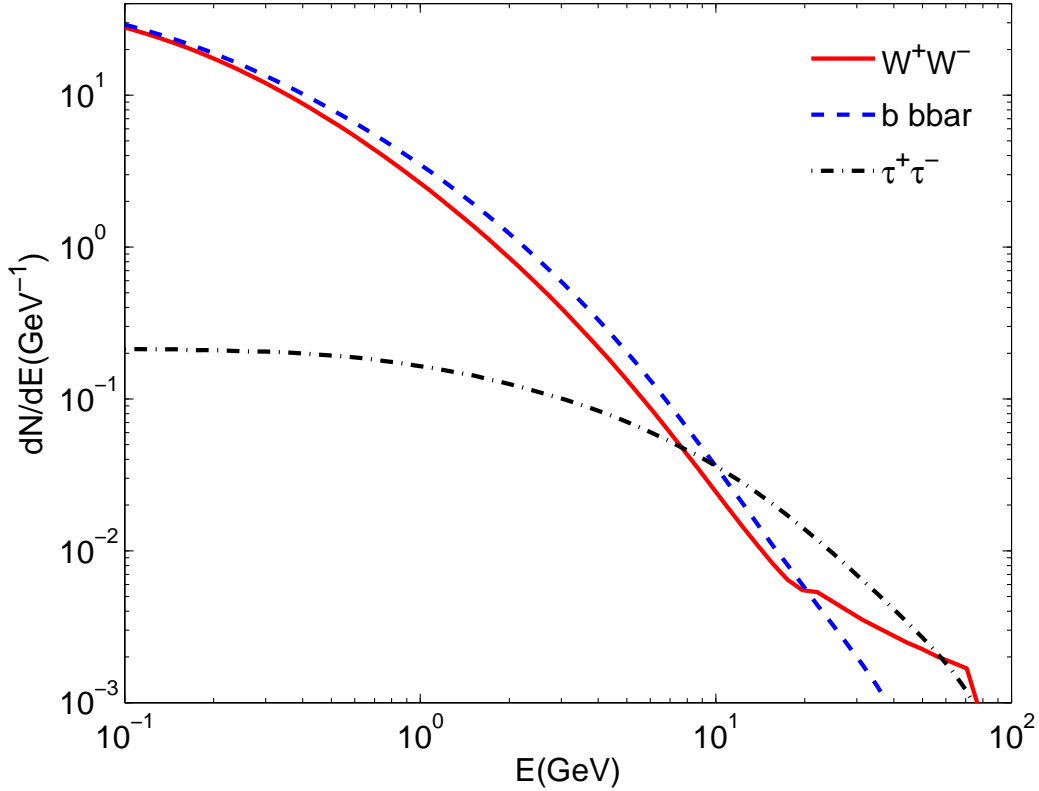


Figure 1: Electron yield spectra dN/dE for W^+W^- , $b\bar{b}$ and $\tau^+\tau^-$ annihilation modes for neutralino with mass $m_{\text{WIMP}} = 100$ GeV.

The annihilation cross section is not well constrained yet. Ref. [55] proposed a very conservative theoretical constraint $\langle\sigma v\rangle \lesssim 10^{-22}(\frac{m_\chi}{1\text{TeV}})^{-2} \text{ cm}^3 \text{ s}^{-1}$. Also there are many constraints from the indirect detection experiments [56, 57, 58], however, all of these results depend strongly on the model, including both the DM models and the astrophysical background estimations. If the WIMP DM is thermally produced in the early universe, the relic density we observe today can provide a fiducial value of the cross section [12]

$$\langle\sigma v\rangle \simeq \frac{3 \times 10^{-27} \text{ cm}^3 \text{ s}^{-1}}{\Omega_\chi h^2}, \quad (3.2)$$

with the DM density $\Omega_\chi h^2 = 0.1143 \pm 0.0034$ from the recent combined analysis of WMAP five year data together with Type Ia supernova and baryon acoustic oscillation data [8]. The DM relic density indicates a cross section $\langle\sigma v\rangle_{\text{WIMP}} \simeq 3 \times 10^{-26} \text{ cm}^3 \text{ s}^{-1}$. Scanning the parameter space of MSSM, we can indeed find a series of models which have such a cross section and satisfy the relic density condition. For clarity we will fix this value of cross section for WIMP DM in the following discussion.

3.2 LDM

The annihilation of LDM with mass 1 – 100 MeV was proposed as the source of the 511 keV line emission in the Galactic center as observed by INTEGRAL [17], though more recent observation and analysis seems to favor a more conventional origin of these electrons [59, 60, 61, 62]. The constraints from COMPTEL and EGRET observations on the γ -rays produced by electromagnetic radiative corrections to $\chi\chi \rightarrow e^+e^-$ process require $m_\chi \lesssim 20$ MeV [18]. More strict mass upper bound of several MeV was found in [21, 22]. Constraints from CMB anisotropy yields similar bound [23]. Other bounds include the value of $g - 2$ [20], big bang nucleosynthesis (BBN) [19]. For such low mass DM particles, the allowed annihilations can only be to e^+e^- , γ -rays and neutrinos. Following [17] we assume that the only annihilation channel of LDM is $\chi\chi \rightarrow e^+e^-$. This assumption means that the annihilation of the LDM is “invisible” to most other observations [18]. The final state electrons are monochrome with energy spectra $dN/dE = \delta(E - m_\chi)$.

The cross section derived from the flux of the 511 keV γ -ray emission is $\langle\sigma v\rangle_{\text{LDM}} \cdot \left(\frac{1 \text{ MeV}}{m_\chi}\right)^2 \sim 10^{-29} - 10^{-30} \text{ cm}^3 \text{ s}^{-1}$ [17], which is consistent with the observational relic density of DM [17]. This LDM cross section must be regarded as an *upper limit* now, as the more detailed analysis show that a large fraction of the Galactic center positrons observed by the INTEGRAL is produced by astrophysical sources [59, 60, 61, 62].

4. Propagation of electrons in cluster

The electrons propagate diffusively in the cluster and experience energy loss processes due to the IC scattering, synchrotron radiation, Coulomb collisions and bremsstrahlung emission. The propagation equation for electrons can be written as

$$\nabla \cdot \left[D(E, \mathbf{r}) \nabla \frac{dn_e}{dE} \right] - \frac{\partial}{\partial E} \left[b(E, \mathbf{r}) \frac{dn_e}{dE} \right] + Q_e(E, \mathbf{r}) = 0, \quad (4.1)$$

where dn_e/dE is the equilibrium electron density distribution, $D(E, \mathbf{r})$ and $b(E, \mathbf{r}) = dE/dt$ are the diffusion coefficient and energy loss rate respectively. For simplicity one can assume $D(E, \mathbf{r})$ and $b(E, \mathbf{r})$ to be independent of the spatial location in the cluster. The diffusion coefficient can be adopted as a power law with respect to electron energy [63]

$$D(E) = D_0 \left(\frac{d_B}{1 \text{ kpc}} \right)^{2/3} \left(\frac{1 \mu\text{G}}{B} \frac{E}{1 \text{ GeV}} \right)^{1/3}, \quad (4.2)$$

where D_0 is a constant, B is the average magnetic field, and d_B is the minimum scale of uniformity of the magnetic field. For Coma, these parameters are estimated as $D_0 \approx 3 \times 10^{28}$

$\text{cm}^2 \text{ s}^{-1}$, $B \approx 1\mu\text{G}$ and $d_B \approx 20 \text{ kpc}$ [26]. The energy loss rate $b(E)$ is [64]

$$\begin{aligned} \frac{b(E)}{10^{-16}\text{GeV s}^{-1}} &= b_{\text{IC}}(E) + b_{\text{syn}}(E) + b_{\text{Coul}}(E) + b_{\text{brem}}(E) \\ &= 0.25 \times \left(\frac{\beta E}{1\text{GeV}}\right)^2 + 0.0254 \times \left(\frac{B}{1\mu\text{G}} \frac{\beta E}{1\text{GeV}}\right)^2 \\ &+ 6.13 \times \left(\frac{1}{\beta} \frac{n}{1\text{cm}^{-3}}\right) \left[1 + 0.013 \ln\left(\gamma \cdot \frac{1\text{cm}^{-3}}{n}\right)\right] \\ &+ 1.39 \times \left(\frac{n}{1\text{cm}^{-3}} \frac{E}{1\text{GeV}}\right) [\ln(2\gamma) - 0.33], \end{aligned} \quad (4.3)$$

where β and γ are the velocity and Lorentz factor of electrons respectively, and n is the number density of the thermal electrons in the cluster as given in Eq.(2.1).

4.1 The diffusionless approximation

In Ref.[26], it was argued that in galaxy clusters the spatial diffusion is negligible compared with energy loss, then Eq.(4.1) has very simple solution

$$\frac{dn_e}{dE} = \frac{1}{b(E)} \int_E^\infty dE' Q_e(E', \mathbf{r}), \quad (4.4)$$

where $Q_e(E, \mathbf{r})$ is the source function given in Eq.(3.1).

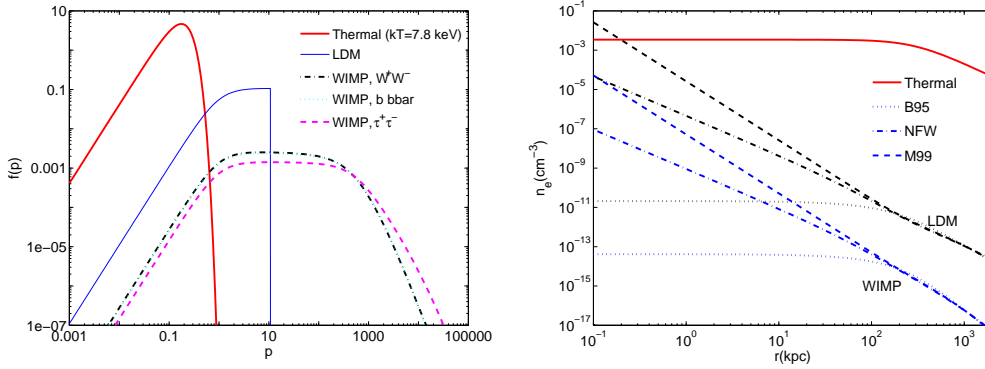


Figure 2: *Left:* normalized equilibrium momentum ($p = \gamma\beta$) spectra of electrons generated from DM annihilation and thermal electrons with $kT_e = 7.8 \text{ keV}$ in Coma cluster. We set $m_{\text{LDM}} = 5 \text{ MeV}$ for LDM and $m_{\text{WIMP}} = 100 \text{ GeV}$ for WIMP. The three typical channels W^+W^- , $b\bar{b}$ and $\tau^+\tau^-$ for neutralino WIMP annihilation are shown respectively. The central value of the thermal electron density is adopted to calculate the energy loss. *Right:* electron density distributions in Coma cluster as functions of radius. Solid line represents the thermal electrons, and the other three lines show the DM induced electrons for B95, NFW and M99 profiles respectively. See the text for details.

In the *left panel* of Figure 2 we show the normalized equilibrium spectrum $f(p) \propto \frac{dn_e}{dE} \frac{dE}{dp}$ of energetic electrons from DM annihilation as a function of dimensionless momentum $p = \gamma\beta$. The masses are adopted as 100 GeV for WIMP and 5 MeV for LDM. For comparison we also plot a thermal electron population with temperature $kT_e = 7.8 \text{ keV}$,

which is the temperature of thermal electrons in the central region of Coma cluster [48]. We see in this figure that at high energies ($E \gtrsim 1$ GeV, $p \gtrsim 10^3$), the spectra are very soft due to the severe energy loss through the IC scattering. For energy $\lesssim 100$ MeV, the Coulomb loss dominates the energy loss processes [26]. From Eq.(4.3) we know that b_{Coul} is approximately a constant for relativistic electrons, and $\propto 1/\beta$ for non-relativistic electrons. Therefore we see in Figure 2 that $f(p)$ is flat for $1 < p < 100$ and decreases for smaller p .

In the *right panel* of Figure 2 we plot the spatial distributions of electrons for both the thermal population and DM annihilation induced population in the Coma cluster. For WIMP DM the parameters are $m_{\text{WIMP}} = 100$ GeV, $\langle\sigma v\rangle_{\text{WIMP}} = 3 \times 10^{-26}$ cm³ s⁻¹, and the annihilation channel is W^+W^- . For LDM we adopt $m_{\text{WIMP}} = 5$ MeV and $\langle\sigma v\rangle_{\text{LDM}} = 2.5 \times 10^{-29}$ cm³ s⁻¹. It is shown that for thermal electrons the central distribution is a flat core, while for NFW and M99 DM scenarios it is strongly cusped in the center. We also note here that at large radius ($\gtrsim 100$ kpc), the electron density decrease less rapidly than expected from the decrease of DM density ($\sim r^{-6}$) because the Coulomb energy loss rate also decreases, thanks to the lower thermal electron density at large radii.

However, even for $r \lesssim 1$ kpc (corresponding to an angular scale $\lesssim 2''$), the density of non-thermal electrons produced by DM annihilation is still several orders of magnitude lower than the thermal one, therefore it would be very difficult or impossible to detect the DM annihilation-induced SZ effect ($\propto n_e$, see Sec. 5). Since the number density of electrons is proportional to $1/m_\chi^2$, the LDM model could generate more electrons, and might be able to produce some observational signals of SZ effect.

4.2 The effect of diffusion

It is known that the overall diffusion time of electrons in galaxy cluster is much longer than the energy loss time [26]. However, if we focus on the local region such as the central part of the cluster, the diffusion term could still be comparable with the energy loss term and may significantly modify the equilibrium electron spectrum and spatial distribution. We now consider this effect.

In this case, using the Green's function method, the solution of the electron density can be written as

$$\frac{dn_e}{dE} = \frac{1}{b(E)} \int_E^\infty dE' G(r, \Delta v) Q_e(E', \mathbf{r}), \quad (4.5)$$

where

$$G(r, \Delta v) = \frac{1}{\sqrt{4\pi\Delta v}} \sum_{n=-\infty}^{+\infty} (-1)^n \int_0^{r_h} dr' \frac{r'}{r_n} \times \left[\exp\left(-\frac{(r' - r_n)^2}{4\Delta v}\right) - \exp\left(-\frac{(r' + r_n)^2}{4\Delta v}\right) \right] \frac{\rho^2(r')}{\rho^2(r)}, \quad (4.6)$$

$r_n = (-1)^n r + 2nr_h$ is the location of the n th ‘‘charge’’ image, r_h is the radius of the diffusion halo, and $\Delta v(E, E') = \int_E^{E'} de D(e)/b(e)$.

In the *left panel* of Figure 3, the momentum spectra of the electrons with the diffusion effect included are shown as lines. For comparison, we also plot the results without diffusion

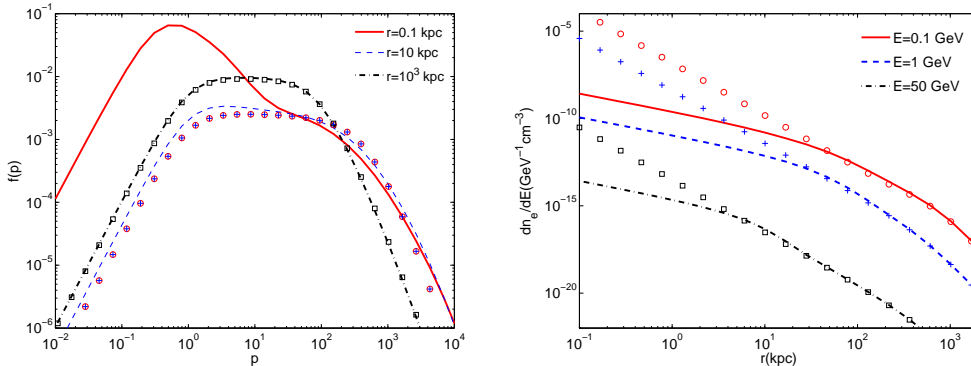


Figure 3: *Left:* the normalized electron spectra $f(p)$ for $r = 0.1, 10$ and 10^3 kpc respectively, compared with the results without diffusion (shown by points with the same colors as the lines). *Right:* the electron density profiles for three energies $E = 0.1, 1$ and 50 GeV, compared with the results without diffusion (points). In this calculation we adopt WIMP DM with W^+W^- channel and M99 density profile. See the text for details.

as points on the same figure. In this calculation we adopt a WIMP DM with mass $m_\chi = 100$ GeV, assuming the W^+W^- channel, and the M99 density profile. We see that the diffusion indeed can lead to distortion of electron spectrum, especially when r is small. For $r \gtrsim 10$ kpc, where the spatial gradient of the DM distribution is small, the effect becomes negligible. The spatial distributions of the electrons for several energies are shown in the *right panel* of Figure 3. It is clear that at small radii diffusion leads to a smoothing of the spatial profile of electrons, while at large radii the results approach the diffusionless solution. We also note that the differences between the cases with and without diffusion are energy-dependent. For higher energy, the energy loss is more important, and the diffusion effect is weaker, so the differences begin to appear at smaller radii for higher energy. An important consequence is that the strong central cusp of electron distribution is smeared out, which significantly affects the SZ effect for high angular resolution observation. Similarly, for the NFW profile there is also a smoothing effect from diffusion. Only in the case of the cored B95 profile the diffusion does not make a difference.

5. SZ effect

For the calculation of SZ effect, we follow the method presented in Ref. [65]. The temperature variation of CMB after traveling through a population of electrons is

$$\frac{\Delta T(x, \theta)}{T_0} = \frac{(e^x - 1)^2}{x^4 e^x} g(x) y(\theta), \quad (5.1)$$

where $x = h\nu/kT_0$ is the dimensionless frequency of CMB photon, $T_0 = 2.725$ K is the undistorted CMB temperature, $g(x)$ is the spectral distortion function, and $y(\theta)$ is the Comptonization parameter which is proportional to the number density of electrons, for angle separation θ from the center. The spectral distortion function can be expressed as

$$g(x) = \frac{m_e c^2}{\langle kT_e \rangle} \left[\int_{-\infty}^{+\infty} i_0(xe^{-s}) P_1(s) ds - i_0(x) \right], \quad (5.2)$$

where $i_0(x) = x^3/(e^x - 1)$ is the Plankian distribution of CMB photons, $s = \ln(\nu'/\nu)$ is the frequency shift of one photon after one scattering with electrons, and $P_1(s)$ is the frequency shift probability distribution,

$$P_1(s) = \int f(p)P_s(s, p)dp, \quad (5.3)$$

with p and $f(p)$ are the dimensionless momentum and momentum spectrum respectively, and $P_s(s, p)$ is the probability of a photon has an energy shift s when colliding with an electron with momentum p [66, 67]. The $\langle kT_e \rangle$ in Eq.(5.2) is the average effective electron temperature defined as [65]

$$\langle kT_e \rangle = \frac{\int P_e dl}{\int n_e dl} = \int \frac{1}{3} f(p) p \beta m_e c^2 dp, \quad (5.4)$$

with P_e the pressure of electrons, and dl the line-of-sight integral. Finally the Comptonization parameter $y(\theta)$ in Eq.(5.1) is given by

$$y(\theta) = \frac{\langle kT_e \rangle}{m_e c^2} \tau = \frac{\langle kT_e \rangle}{m_e c^2} \cdot \sigma_T \int n_e dl, \quad (5.5)$$

where σ_T is the Thomson cross section. For the case with diffusion effect, the spatial and energy distributions of electrons are coupled together, $g(x)y(\theta)$ is integrated together in the line-of-sight integral.

Since the DM induced electrons will concentrate near the center of the cluster for cuspy density profiles, while from the observational point of view we only have limited resolution angle, it is necessary to smooth the results within the resolution angle of the detector array. In Figure 4 we show the average Comptonization parameter, $y_{\text{sm}}(\theta_{\text{sm}}) = \frac{\int_0^{\theta_{\text{sm}}} \theta y(\theta) d\theta}{\int_0^{\theta_{\text{sm}}} \theta d\theta}$, as a function of the beam size angle θ_{sm} for the WIMP DM. It is shown that for the diffusionless case y_{sm} varies approximately with θ_{sm}^0 , θ_{sm}^{-1} and θ_{sm}^{-2} for B95, NFW and M99 profiles respectively. For the case with diffusion the central cusp of electrons from NFW and M99 profiles are smoothed out and the angle dependence of y_{sm} becomes much weaker.

The expected temperature variation of CMB due to the e^+e^- from DM annihilation in Coma cluster is shown in Figure 5. The left panel is for WIMP with mass $m_{\text{WIMP}} = 100$ GeV and annihilation channel W^+W^- ; the right panel is for LDM with $m_{\text{LDM}} = 5$ MeV. The beam width is assumed to be 1 arcsec around the center of the cluster, which corresponds to a radial distance ~ 0.5 kpc from the center. In each panel, we plot the thermal SZ effect as a solid red curve (on the left panel, due to the scale of the plot, it appears as almost a vertical line). The DM-induced SZ effect for the M99 profile without inclusion of diffusion is shown as open circles, the DM-induced SZ effect for the M99 profile with diffusion as blue dashed curves. The effect for the NFW and B95 profiles are also plotted, though as they are much smaller compared with the more cuspy M99 profile, the two curves almost coincides with the x-axis and are hardly visible.

We can see that for typical WIMPs (left panel of Fig. 5) the DM-induced SZ effect is extremely small. At 217 GHz ($x \approx 3.83$) where the thermal SZ effect is zero, even without including the effect of diffusion, the DM-induced SZ effect for the M99 profile is only

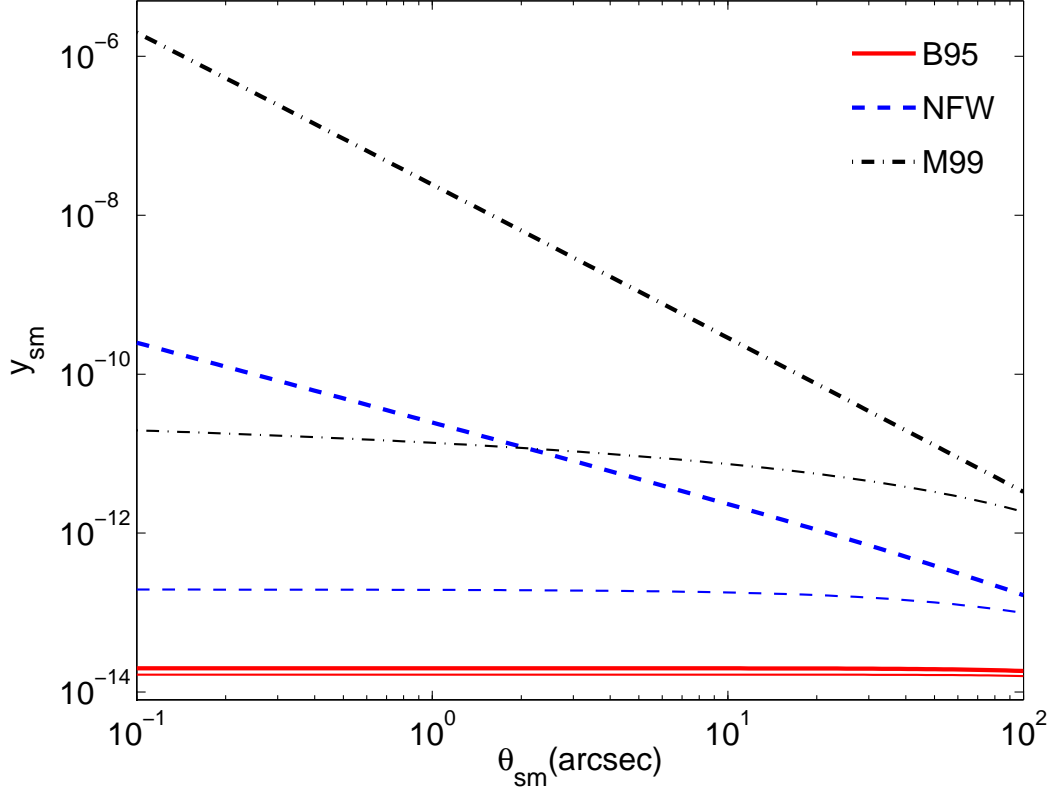


Figure 4: Smoothed Comptonization parameter for WIMP as a function of the smooth angle θ_{sm} for B95, NFW and M99 density profiles respectively. The thick lines show the results without diffusion effect, and the thin lines are the cases with diffusion effect.

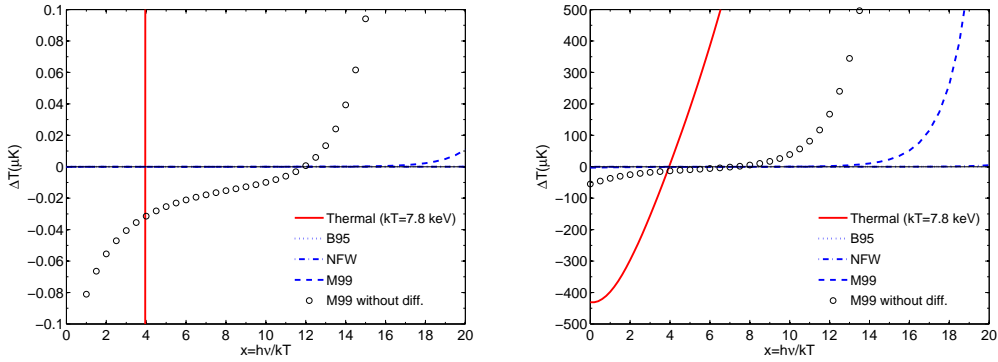


Figure 5: CMB temperature variation due to the e^+e^- from DM annihilation in Coma cluster. *Left panel* is for WIMP with mass $m_{\text{WIMP}} = 100$ GeV (W^+W^- channel), and *right panel* is for LDM with $m_{\text{LDM}} = 5$ MeV. See text for detail.

$-3 \times 10^{-2} \mu\text{K}$. These results are much smaller than those given in [24, 26]². While we have

²Note that in a recent study similar conclusion is also derived [68].

adopted different parameter values in the the models presented above, we have also checked the cases given in [26], i.e., N04 density profile [33], $m_\chi = 40$ GeV, $\sigma v = 4.7 \times 10^{-25} \text{ cm}^3 \text{ s}^{-1}$ and $b\bar{b}$ annihilation channel. We find that the temperature variation to be $\sim 3 \times 10^{-2} \mu\text{K}$ for frequency 30GHz, which is about three orders of magnitude lower than the result of $\sim 40 \mu\text{K}$ given in Ref.[26].

For the case of LDM (see right panel of Fig. 5), the DM induced SZ effect is larger. In the diffusionless approximation, at frequency 217 GHz, for example, the temperature deviations for M99 profile is $-16 \mu\text{K}$, which is comparable with the sensitivity of the next generation SZ interferometer such as the Atacama Large Millimeter Array (ALMA)³.

However, with the effect of diffusion which lowers the density of electron-positron pairs near the center of the cluster, the DM-induced SZ effect is even smaller. For WIMP, even for the M99 profile, it is only $-2 \times 10^{-5} \mu\text{K}$ (about $10^{-7} \mu\text{K}$ for NFW profile, $10^{-8} \mu\text{K}$ for B95 profile). For LDM, although it is larger than the WIMP case, the DM-induced SZ effect is only $-0.75 \mu\text{K}$ for the M99 profile, making its detection extremely difficult if not impossible.

Finally we plot in Figure 6 the calculated SZ effects for the 9 clusters given in Table 1. The DM profile is adopted as M99 and the results are smoothed within 1 arcsec around the center of the halo. Note that the non-thermal SZ effect from DM annihilation is more remarkable for nearby clusters, because for far away clusters the same beam size will correspond to a larger region around the center, and the average effect becomes smaller. We can see that if the diffusion effects are taken into account, there is almost no chance to detect the DM induced SZ effects due to the very weak signals and strong thermal backgrounds.

6. Discussion

In this work we calculate the SZ effect induced by e^+e^- from DM annihilation in galaxy clusters. Two types of DM particles, WIMP and LDM, are considered. The annihilation cross sections we adopted satisfy the constraint from the relic density of DM. Neutralino in the framework of supersymmetry is taken as an example of WIMP DM, and three typical annihilation channels, W^+W^- , $b\bar{b}$ and $\tau^+\tau^-$ are employed. For LDM we assume the only annihilation channel is e^+e^- , and its annihilation cross cross to produce all of the positrons in the Galactic center, which should be regarded as very conservative upper limits. The density profile of DM halo is a crucial factor, and we consider the Burkert, NFW and Moore profiles to represent the case of non-cuspy, medately cuspy and strongly cuspy profiles respectively.

We find much smaller (two orders of magnitude or more) DM-induced SZ effect than previous claims for WIMPs. Furthermore, we consider the spatial diffusion of electrons, which was negelected in previous works. This effect significantly reduced the density of energetic electrons in the center of halo, especially for the DM profile with strong cusp. Due to this effect, the DM induced SZ effect is even weaker. For WIMPs, the DM induced

³<http://www.eso.org/sci/facilities/alma/index.html>

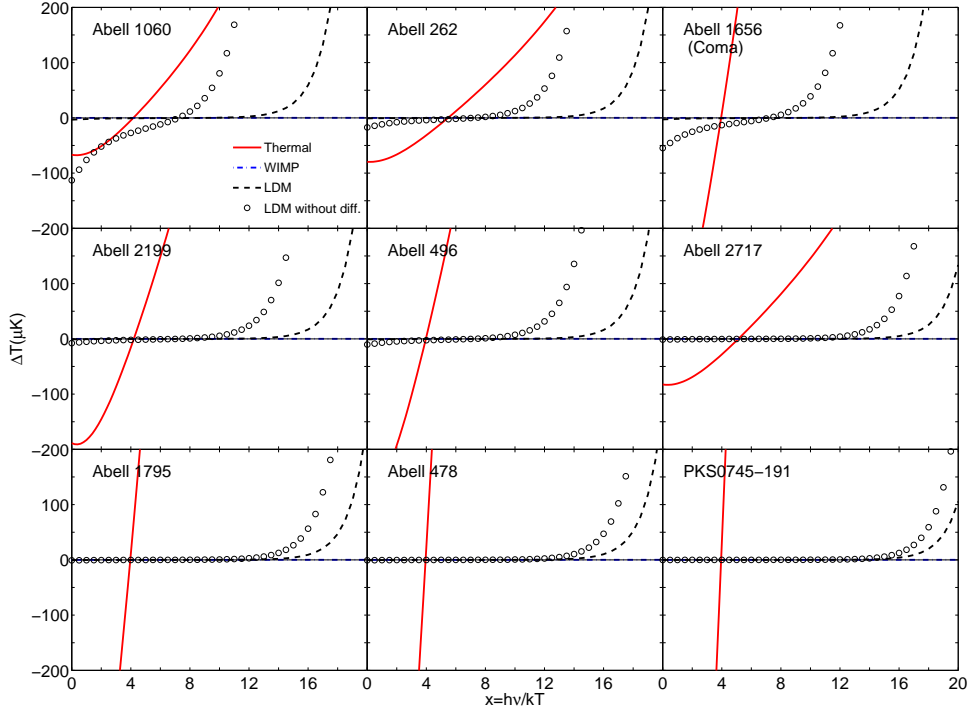


Figure 6: Temperature variations of CMB due to the e^+e^- from DM annihilation for the 9 clusters listed in Table 1. The masses of WIMP and LDM are 100 GeV and 5 MeV respectively, and the DM profile is M99.

SZ effect is several orders of magnitude smaller than the thermal one. Although the LDM could produce stronger signal than the WIMPs, it is still very small. Given the small size of the DM-induced SZ signal, not to mention the practical issues of separating the signal from possible confusions such as astrophysical foreground, kinetic SZ effect, and fluctuation of primordial CMB temperature, we conclude that it would be extremely difficult if not entirely impossible to detect the DM induced SZ effect with the next generation SZ interferometer such as ALMA.

There are large uncertainties about the particle physics properties of DM such as the mass and annihilation cross section. For WIMP, we fix the cross section to be $\langle\sigma v\rangle_{\text{WIMP}} \simeq 3 \times 10^{-26} \text{ cm}^3 \text{ s}^{-1}$ taking into account the constraint from the relic density, so the SZ effect will be approximately proportional to $1/m_{\text{WIMP}}^2$. For lower mass WIMPs, the SZ effect can be stronger. Furthermore, larger cross section is also possible in some scenarios such as the non-thermal production of DM or the ‘‘Sommerfeld enhancement’’ [69, 70, 71, 72, 73], but these scenarios is constrained by, e.g., the γ -rays [74, 75]. For LDM, since the annihilation cross section derived from the 511 keV observations at the Galactic center scales as m_{LDM}^2 , the change of electron density through varying m_{LDM}^2 is compensated by a rescaled cross section. However, different mass will result in different high energy cut off for the equi-

librium electron spectrum (Eq.(4.4)) and the eventual SZ effect would be affected⁴. More quantitatively we find that the temperature distortion is nearly proportional to m_{LDM} . Since the mass of LDM is constrained in a narrow range by other methods [18, 20, 21, 23], we think the basic conclusion of this work is still valid.

The DM substructures inside the halo might also “boost” the annihilation signal [76, 77, 78]. However, the substructures near the center of the halo would be destroyed by the tidal force, and the “boost” can only take effect at large radii [79]. Furthermore, for the cuspy profiles the central density is high enough to dominate the contribution over that from substructures, hence the “boost” effect is relatively weak. Therefore if we investigate the SZ effect at the center of the cluster, the effect of substructures can be reasonably neglected.

Finally we note that the recent observations of the electrons/positrons by ATIC and PAMELA experiments show apparent excesses of energetic electron/positrons compared with the conventional cosmic ray model predictions [80, 81]. If these excesses are ascribed to DM annihilation, the mass of DM particle $\gtrsim 700$ GeV and a boost factor of order $\sim 10^2$ are needed, and the annihilation modes should be lepton dominated (e.g., Ref. [82]). We also calculate the SZ effect of this DM configuration, and find that the results are almost the same as the 100 GeV WIMP used in this work. This is mainly because the boost factor is canceled by the $1/m_\chi^2$ term. That is to say, the SZ effect from DM annihilation is still very difficult to be detected even for the enhanced electron/positron density as required by ATIC and PAMELA.

Acknowledgments

We thank S. Colafrancesco, P. Ullio and Pengjie Zhang for helpful discussions. Qiang Yuan thanks Juan Zhang and Jiajie Gao for help on the calculations. This work is supported by the National Science Foundation of China under grants 10575111, 10773011, 10525314, 10533010, by the Chinese Academy of Sciences under grant No. KJCX3-SYW-N2, and by the Ministry of Science and Technology National Basic Science Program (Project 973) under grant No.2007CB815401.

References

- [1] F. Zwicky, *Die Rotverschiebung von extragalaktischen Nebeln*, *Helvetica Physica Acta* **6** (1933) 110–127.
- [2] K. G. Begeman, A. H. Broeils, and R. H. Sanders, *Extended rotation curves of spiral galaxies - Dark haloes and modified dynamics*, *Mon. Not. Roy. Astron. Soc.* **249** (Apr., 1991) 523–537.
- [3] S. D. M. White, J. F. Navarro, A. E. Evrard, and C. S. Frenk, *The Baryon Content of Galaxy Clusters - a Challenge to Cosmological Orthodoxy*, *Nature* **366** (Dec., 1993) 429.

⁴This effect does not affect the WIMP case. From Figure 2 we can see that the equilibrium electron spectrum is insensitive to the high energy cutoff in the spectrum due to the fast IC energy loss.

- [4] J. A. Tyson and P. Fischer, *Measurement of the Mass Profile of Abell 1689*, *Astrophys. J. Lett.* **446** (June, 1995) L55, [astro-ph/].
- [5] M. Tegmark, M. R. Blanton, M. A. Strauss, F. Hoyle, D. Schlegel, R. Scoccimarro, M. S. Vogeley, D. H. Weinberg, I. Zehavi, A. Berlind, T. Budavari, A. Connolly, D. J. Eisenstein, D. Finkbeiner, J. A. Frieman, J. E. Gunn, A. J. S. Hamilton, L. Hui, B. Jain, D. Johnston, S. Kent, H. Lin, R. Nakajima, R. C. Nichol, J. P. Ostriker, A. Pope, R. Scranton, U. Seljak, R. K. Sheth, A. Stebbins, A. S. Szalay, I. Szapudi, L. Verde, Y. Xu, J. Annis, N. A. Bahcall, J. Brinkmann, S. Burles, F. J. Castander, I. Csabai, J. Loveday, M. Doi, M. Fukugita, J. R. I. Gott, G. Hennessy, D. W. Hogg, Ž. Ivezić, G. R. Knapp, D. Q. Lamb, B. C. Lee, R. H. Lupton, T. A. McKay, P. Kunszt, J. A. Munn, L. O’Connell, J. Peoples, J. R. Pier, M. Richmond, C. Rockosi, D. P. Schneider, C. Stoughton, D. L. Tucker, D. E. Vanden Berk, B. Yanny, and D. G. York, *The Three-Dimensional Power Spectrum of Galaxies from the Sloan Digital Sky Survey*, *Astrophys. J.* **606** (May, 2004) 702–740, [astro-ph/].
- [6] P. de Bernardis, P. A. R. Ade, J. J. Bock, J. R. Bond, J. Borrill, A. Boscaleri, K. Coble, B. P. Crill, G. De Gasperis, P. C. Farese, P. G. Ferreira, K. Ganga, M. Giacometti, E. Hivon, V. V. Hristov, A. Iacoangeli, A. H. Jaffe, A. E. Lange, L. Martinis, S. Masi, P. V. Mason, P. D. Mauskopf, A. Melchiorri, L. Miglio, T. Montroy, C. B. Netterfield, E. Pascale, F. Piacentini, D. Pogosyan, S. Prunet, S. Rao, G. Romeo, J. E. Ruhl, F. Scaramuzzi, D. Sforna, and N. Vittorio, *A flat Universe from high-resolution maps of the cosmic microwave background radiation*, *Nature* **404** (Apr., 2000) 955–959, [astro-ph/].
- [7] D. N. Spergel, L. Verde, H. V. Peiris, E. Komatsu, M. R. Nolta, C. L. Bennett, M. Halpern, G. Hinshaw, N. Jarosik, A. Kogut, M. Limon, S. S. Meyer, L. Page, G. S. Tucker, J. L. Weiland, E. Wollack, and E. L. Wright, *First-Year Wilkinson Microwave Anisotropy Probe (WMAP) Observations: Determination of Cosmological Parameters*, *Astrophys. J. Supp.* **148** (Sept., 2003) 175–194, [astro-ph/].
- [8] E. Komatsu, J. Dunkley, M. R. Nolta, C. L. Bennett, B. Gold, G. Hinshaw, N. Jarosik, D. Larson, M. Limon, L. Page, D. N. Spergel, M. Halpern, R. S. Hill, A. Kogut, S. S. Meyer, G. S. Tucker, J. L. Weiland, E. Wollack, and E. L. Wright, *Five-Year Wilkinson Microwave Anisotropy Probe Observations: Cosmological Interpretation*, *Astrophys. J. Supp.* **180** (Feb., 2009) 330–376, [arXiv:0803.0547].
- [9] T. P. Walker, G. Steigman, H.-S. Kang, D. M. Schramm, and K. A. Olive, *Primordial nucleosynthesis redux*, *Astrophys. J.* **376** (July, 1991) 51–69.
- [10] M. S. Smith, L. H. Kawano, and R. A. Malaney, *Experimental, computational, and observational analysis of primordial nucleosynthesis*, *Astrophys. J. Supp.* **85** (Apr., 1993) 219–247.
- [11] M. Davis, G. Efstathiou, C. S. Frenk, and S. D. M. White, *The evolution of large-scale structure in a universe dominated by cold dark matter*, *Astrophys. J.* **292** (May, 1985) 371–394.
- [12] G. Jungman, M. Kamionkowski, and K. Griest, *Supersymmetric dark matter*, *Phys. Rept.* **267** (Mar., 1996) 195–373, [hep-ph/95].
- [13] G. Bertone, D. Hooper, and J. Silk, *Particle dark matter: evidence, candidates and constraints.*, *Phys. Rept.* **405** (2004) 279–390.
- [14] D. Hooper and T. Plehn, *Supersymmetric dark matter-how light can the LSP be?*, *Physics Letters B* **562** (June, 2003) 18–27, [hep-ph/02].

- [15] C. Boehm, T. A. Enßlin, and J. Silk, *Can annihilating dark matter be lighter than a few GeVs?*, *Journal of Physics G Nuclear Physics* **30** (Mar., 2004) 279–285, [astro-ph/].
- [16] C. Boehm and P. Fayet, *Scalar dark matter candidates*, *Nuclear Physics B* **683** (Apr., 2004) 219–263, [hep-ph/03].
- [17] C. Boehm, D. Hooper, J. Silk, M. Casse, and J. Paul, *MeV Dark Matter: Has It Been Detected?*, *Physical Review Letters* **92** (Mar., 2004) 101301, [astro-ph/].
- [18] J. F. Beacom, N. F. Bell, and G. Bertone, *Gamma-Ray Constraint on Galactic Positron Production by MeV Dark Matter*, *Physical Review Letters* **94** (May, 2005) 171301, [astro-ph/].
- [19] P. D. Serpico and G. G. Raffelt, *MeV-mass dark matter and primordial nucleosynthesis*, *Phys. Rev. D* **70** (Aug., 2004) 043526+, [astro-ph/].
- [20] Y. Ascasibar, P. Jean, C. Boehm, and J. Knödseder, *Constraints on dark matter and the shape of the Milky Way dark halo from the 511-keV line*, *Mon. Not. Roy. Astron. Soc.* **368** (June, 2006) 1695–1705, [astro-ph/].
- [21] P. Sizun, M. Cassé, and S. Schanne, *Continuum γ -ray emission from light dark matter positrons and electrons*, *Phys. Rev. D* **74** (Sept., 2006) 063514, [astro-ph/].
- [22] J. F. Beacom and H. Yüksel, *Stringent Constraint on Galactic Positron Production*, *Physical Review Letters* **97** (Aug., 2006) 071102+, [astro-ph/].
- [23] L. Zhang, X. Chen, Y.-A. Lei, and Z.-G. Si, *Impacts of dark matter particle annihilation on recombination and the anisotropies of the cosmic microwave background*, *Phys. Rev. D* **74** (Nov., 2006) 103519, [astro-ph/].
- [24] S. Colafrancesco, *SZ effect from Dark Matter annihilation*, *Astron. Astrophys.* **422** (July, 2004) L23–L27, [astro-ph/].
- [25] T. L. Culverhouse, N. W. Evans, and S. Colafrancesco, *Comptonization of cosmic microwave background photons in dwarf spheroidal galaxies*, *Mon. Not. Roy. Astron. Soc.* **368** (May, 2006) 659–667, [astro-ph/].
- [26] S. Colafrancesco, S. Profumo, and P. Ullio, *Multi-frequency analysis of neutralino dark matter annihilations in the Coma cluster*, *Astron. Astrophys.* **455** (Aug., 2006) 21–43, [astro-ph/].
- [27] S. Colafrancesco, S. Profumo, and P. Ullio, *Detecting dark matter WIMPs in the Draco dwarf: A multiwavelength perspective*, *Phys. Rev. D* **75** (Jan., 2007) 023513, [astro-ph/].
- [28] S. Colafrancesco, P. de Bernardis, S. Masi, G. Polenta, and P. Ullio, *Direct probes of dark matter in the cluster 1ES0657-556 through microwave observations*, *Astron. Astrophys.* **467** (May, 2007) L1–L5, [astro-ph/].
- [29] A. Cavaliere and R. Fusco-Femiano, *X-rays from hot plasma in clusters of galaxies*, *Astron. Astrophys.* **49** (May, 1976) 137–144.
- [30] C. L. Sarazin, *X-ray emission from clusters of galaxies*. Cambridge Astrophysics Series, Cambridge: Cambridge University Press, 1988, 1988.
- [31] J. F. Navarro, C. S. Frenk, and S. D. M. White, *A Universal Density Profile from Hierarchical Clustering*, *Astrophys. J.* **490** (Dec., 1997) 493, [astro-ph/].
- [32] B. Moore, F. Governato, T. Quinn, J. Stadel, and G. Lake, *Resolving the Structure of Cold Dark Matter Halos*, *Astrophys. J. Lett.* **499** (May, 1998) L5, [astro-ph/].

- [33] J. F. Navarro, E. Hayashi, C. Power, A. R. Jenkins, C. S. Frenk, S. D. M. White, V. Springel, J. Stadel, and T. R. Quinn, *The inner structure of Λ CDM haloes - III. Universality and asymptotic slopes*, *Mon. Not. Roy. Astron. Soc.* **349** (Apr., 2004) 1039–1051, [astro-ph/].
- [34] J. Diemand, B. Moore, and J. Stadel, *Earth-mass dark-matter haloes as the first structures in the early Universe*, *Nature* **433** (Jan., 2005) 389–391, [astro-ph/].
- [35] B. Moore, *Evidence against Dissipationless Dark Matter from Observations of Galaxy Haloes*, *Nature* **370** (Aug., 1994) 629.
- [36] A. Burkert, *The Structure of Dark Matter Halos in Dwarf Galaxies*, *Astrophys. J. Lett.* **447** (July, 1995) L25, [astro-ph/].
- [37] P. Salucci, A. Lapi, C. Tonini, G. Gentile, I. Yegorova, and U. Klein, *The universal rotation curve of spiral galaxies - II. The dark matter distribution out to the virial radius*, *Mon. Not. Roy. Astron. Soc.* **378** (June, 2007) 41–47, [astro-ph/].
- [38] A. Cooray and R. Sheth, *Halo models of large scale structure*, *Phys. Rept.* **372** (Dec., 2002) 1–129, [astro-ph/].
- [39] B. Moore, T. Quinn, F. Governato, J. Stadel, and G. Lake, *Cold collapse and the core catastrophe*, *Mon. Not. Roy. Astron. Soc.* **310** (Dec., 1999) 1147–1152, [astro-ph/].
- [40] V. S. Berezinsky, A. V. Gurevich, and K. P. Zybin, *Distribution of dark matter in the Galaxy and the lower limits for the masses of supersymmetric particles.*, *Physics Letters B* **294** (Nov., 1992) 221–228.
- [41] J. Lavalle, Q. Yuan, D. Maurin, and X. J. Bi, *Full calculation of clumpiness boost factors for antimatter cosmic rays in the light of Λ CDM N-body simulation results. Abandoning hope in clumpiness enhancement?*, *Astron. Astrophys.* **479** (Feb., 2008) 427–452, [0709.3634].
- [42] J. S. Bullock, T. S. Kolatt, Y. Sigad, R. S. Somerville, A. V. Kravtsov, A. A. Klypin, J. R. Primack, and A. Dekel, *Profiles of dark haloes: evolution, scatter and environment*, *Mon. Not. Roy. Astron. Soc.* **321** (Mar., 2001) 559–575, [astro-ph/].
- [43] G. L. Bryan and M. L. Norman, *Statistical Properties of X-Ray Clusters: Analytic and Numerical Comparisons*, *Astrophys. J.* **495** (Mar., 1998) 80, [astro-ph/].
- [44] V. R. Eke, J. F. Navarro, and M. Steinmetz, *The Power Spectrum Dependence of Dark Matter Halo Concentrations*, *Astrophys. J.* **554** (June, 2001) 114–125, [astro-ph/].
- [45] J. M. Comerford and P. Natarajan, *The observed concentration-mass relation for galaxy clusters*, *Mon. Not. Roy. Astron. Soc.* **379** (July, 2007) 190–200, [astro-ph/].
- [46] E. J. Lloyd-Davies, T. J. Ponman, and D. B. Cannon, *The entropy and energy of intergalactic gas in galaxy clusters*, *Mon. Not. Roy. Astron. Soc.* **315** (July, 2000) 689–702, [astro-ph/].
- [47] E. L. Lokas, R. Wojtak, S. Gottlöber, G. A. Mamon, and F. Prada, *Mass distribution in nearby Abell clusters*, *Mon. Not. Roy. Astron. Soc.* **367** (Apr., 2006) 1463–1472, [astro-ph/].
- [48] U. G. Briel, J. P. Henry, and H. Boehringer, *Observation of the Coma cluster of galaxies with ROSAT during the all-sky survey*, *Astron. Astrophys.* **259** (June, 1992) L31–L34.
- [49] K. Rines, M. J. Geller, M. J. Kurtz, and A. Diaferio, *CAIRNS: The Cluster and Infall Region Nearby Survey. I. Redshifts and Mass Profiles*, *Astron. J.* **126** (Nov., 2003) 2152–2170, [astro-ph/].

- [50] H. Liang, M. Pierre, A. Unewisse, and R. W. Hunstead, *An X-ray and radio study of the cluster A 2717.*, *Astron. Astrophys.* **321** (May, 1997) 64–70, [astro-ph/].
- [51] E. Pointecouteau, M. Arnaud, and G. W. Pratt, *The structural and scaling properties of nearby galaxy clusters. I. The universal mass profile*, *Astron. Astrophys.* **435** (May, 2005) 1–7, [astro-ph/].
- [52] R. W. Schmidt and S. W. Allen, *The dark matter haloes of massive, relaxed galaxy clusters observed with Chandra*, *Mon. Not. Roy. Astron. Soc.* **379** (July, 2007) 209–221, [astro-ph/].
- [53] Y. Chen, Y. Ikebe, and H. Böhringer, *X-ray spectroscopy of the cluster of galaxies ζ ASTROBJ/PKS 0745-191/ ζ ASTROBJ with XMM-Newton*, *Astron. Astrophys.* **407** (Aug., 2003) 41–50.
- [54] P. Gondolo, J. Edsjö, P. Ullio, L. Bergström, M. Schelke, and E. A. Baltz, *DarkSUSY: computing supersymmetric dark matter properties numerically*, *Journal of Cosmology and Astro-Particle Physics* **7** (July, 2004) 8, [astro-ph/].
- [55] S. Profumo, *TeV γ -rays and the largest masses and annihilation cross sections of neutralino dark matter*, *Phys. Rev. D* **72** (Nov., 2005) 103521, [astro-ph/].
- [56] G. Zaharijas and D. Hooper, *Challenges in detecting gamma-rays from dark matter annihilations in the galactic center*, *Phys. Rev. D* **73** (May, 2006) 103501, [astro-ph/].
- [57] X. J. Bi, *Constraining supersymmetry from the satellite experiments*, *Phys. Rev. D* **76** (Dec., 2007) 123511, [arXiv:0708.1206].
- [58] D. Hooper, *Constraining supersymmetric dark matter with synchrotron measurements*, *Phys. Rev. D* **77** (June, 2008) 123523, [arXiv:0801.4378].
- [59] G. Weidenspointner, J. Knödlseider, P. Jean, G. K. Skinner, P. von Ballmoos, J.-P. Roques, G. Vedrenne, P. Milne, B. J. Teegarden, R. Diehl, A. Strong, S. Schanne, B. Cordier, and C. Winkler, *The Sky Distribution of 511 keV Positron Annihilation Line Emission as Measured with INTEGRAL/SP125*, in *ESA Special Publication*, vol. 622 of *ESA Special Publication*, p. 25, 2007.
- [60] G. Weidenspointner *et. al.*, *An asymmetric distribution of positrons in the Galactic disk revealed by γ -rays*, *Nature* **451** (2008) 159–162.
- [61] R. M. Bandyopadhyay, J. Silk, J. E. Taylor, and T. J. Maccarone, *On the origin of the 511-keV emission in the Galactic Centre*, *Mon. Not. Roy. Astron. Soc.* **392** (Jan., 2009) 1115–1123, [arXiv:0810.3674].
- [62] R. Diehl and M. Leising, *Gamma-Rays from Positron Annihilation*, *ArXiv e-prints* (June, 2009) [arXiv:0906.1503].
- [63] S. Colafrancesco and P. Blasi, *Clusters of galaxies and the diffuse gamma-ray background*, *Astroparticle Physics* **9** (Oct., 1998) 227–246, [astro-ph/].
- [64] A. W. Strong and I. V. Moskalenko, *Propagation of Cosmic-Ray Nucleons in the Galaxy*, *Astrophys. J.* **509** (Dec., 1998) 212–228, [astro-ph/].
- [65] S. Colafrancesco, P. Marchegiani, and E. Palladino, *The non-thermal Sunyaev-Zel’dovich effect in clusters of galaxies*, *Astron. Astrophys.* **397** (Jan., 2003) 27–52, [astro-ph/].
- [66] M. Birkinshaw, *The Sunyaev-Zel’dovich effect*, *Phys. Rept.* **310** (Mar., 1999) 97–195, [astro-ph/].

- [67] T. A. Enßlin and C. R. Kaiser, *Comptonization of the cosmic microwave background by relativistic plasma*, *Astron. Astrophys.* **360** (Aug., 2000) 417–430, [astro-ph/].
- [68] J. Lavalle, C. Boehm, and J. Barthes, *On the Sunyaev-Zel'dovich effect from dark matter annihilation or decay in galaxy clusters*, *ArXiv e-prints* (July, 2009) [arXiv:0907.5589].
- [69] M. Cirelli, M. Kadastik, M. Raidal, and A. Strumia, *Model-independent implications of the e^+e^- , $p\bar{p}$ cosmic ray spectra on properties of Dark Matter*, *Nuclear Physics B* **813** (May, 2009) 1–2, [arXiv:0809.2409].
- [70] N. Arkani-Hamed, D. P. Finkbeiner, T. R. Slatyer, and N. Weiner, *A theory of dark matter*, *Phys. Rev. D* **79** (Jan., 2009) 015014, [arXiv:0810.0713].
- [71] M. Pospelov and A. Ritz, *Astrophysical signatures of secluded dark matter*, *Physics Letters B* **671** (Jan., 2009) 391–397, [arXiv:0810.1502].
- [72] J. March-Russell, S. M. West, D. Cumberbatch, and D. Hooper, *Heavy dark matter through the Higgs portal*, *Journal of High Energy Physics* **7** (July, 2008) 58, [arXiv:0801.3440].
- [73] J. March-Russell and S. M. West, *WIMPonium and Boost Factors for Indirect Dark Matter Detection*, *ArXiv e-prints* (Dec., 2008) [arXiv:0812.0559].
- [74] M. Kamionkowski and S. Profumo, *Early Annihilation and Diffuse Backgrounds in Models of Weakly Interacting Massive Particles in Which the Cross Section for Pair Annihilation Is Enhanced by $1/v$* , *Physical Review Letters* **101** (Dec., 2008) 261301, [arXiv:0810.3233].
- [75] N. F. Bell and T. D. Jacques, *Gamma-ray Constraints on Dark Matter Annihilation into Charged Particles*, *ArXiv e-prints* (Nov., 2008) [arXiv:0811.0821].
- [76] Q. Yuan and X. J. Bi, *The galactic positron flux and dark matter substructures*, *Journal of Cosmology and Astro-Particle Physics* **5** (May, 2007) 1, [astro-ph/].
- [77] X. J. Bi, J. Zhang, and Q. Yuan, *Diffuse γ rays and \bar{p} flux from dark matter annihilation: A model for consistent results with EGRET and cosmic ray data*, *Phys. Rev. D* **78** (Aug., 2008) 043001, [0712.4038].
- [78] X. J. Bi, J. Zhang, Q. Yuan, J. L. Zhang, and H. S. Zhao, *The diffuse Galactic γ -rays from dark matter annihilation*, *Physics Letters B* **668** (Oct., 2008) 87–92.
- [79] X. J. Bi, *Gamma rays from the neutralino dark matter annihilations in the Milky Way substructures*, *Nuclear Physics B* **741** (May, 2006) 83–107, [astro-ph/].
- [80] J. Chang, J. H. Adams, H. S. Ahn, G. L. Bashindzhagyan, M. Christl, O. Ganel, T. G. Guzik, J. Isbert, K. C. Kim, E. N. Kuznetsov, M. I. Panasyuk, A. D. Panov, W. K. H. Schmidt, E. S. Seo, N. V. Sokolskaya, J. W. Watts, J. P. Wefel, J. Wu, and V. I. Zatsepin, *An excess of cosmic ray electrons at energies of 300-800GeV*, *Nature* **456** (Nov., 2008) 362–365.
- [81] O. Adriani, G. C. Barbarino, G. A. Bazilevskaia, R. Bellotti, M. Boezio, E. A. Bogomolov, L. Bonechi, M. Bongii, V. Bonvicini, S. Bottai, A. Bruno, F. Cafagna, D. Campana, P. Carlson, M. Casolino, G. Castellini, M. P. de Pascale, G. de Rosa, N. de Simone, V. di Felice, A. M. Galper, L. Grishantseva, P. Hofverberg, S. V. Koldashov, S. Y. Krutkov, A. N. Kvashmin, A. Leonov, V. Malvezzi, L. Marcelli, W. Menn, V. V. Mikhailov, E. Mocchiutti, S. Orsi, G. Osteria, P. Papini, M. Pearce, P. Picozza, M. Ricci, S. B. Ricciarini, M. Simon, R. Sparvoli, P. Spillantini, Y. I. Stozhkov, A. Vacchi, E. Vannuccini, G. Vasilyev, S. A. Voronov, Y. T. Yurkin, G. Zampa, N. Zampa, and V. G. Zverev, *An anomalous positron abundance in cosmic rays with energies 1.5-100GeV*, *Nature* **458** (Apr., 2009) 607–609, [arXiv:0810.4995].

- [82] I. Cholis, G. Dobler, D. P. Finkbeiner, L. Goodenough, and N. Weiner, *The Case for a 700+ GeV WIMP: Cosmic Ray Spectra from ATIC and PAMELA*, *ArXiv e-prints* (Nov., 2008) [[arXiv:0811.3641](#)].